



Article

Electrochemical Detection of Bisphenol A by Tyrosinase Immobilized on Electrospun Nanofibers Decorated with Gold Nanoparticles

Luiza A. Mercante^{1,2,*} , Leonardo E. O. Iwaki³, Vanessa P. Scagion^{1,4}, Osvaldo N. Oliveira Jr.³, Luiz H. C. Mattoso¹ and Daniel S. Correa^{1,4,*} 

- ¹ Nanotechnology National Laboratory for Agriculture (LNNA), Embrapa Instrumentação, São Carlos, SP 13560-970, Brazil; vanessa.scagion@gmail.com (V.P.S.); luiz.mattoso@embrapa.br (L.H.C.M.)
² Institute of Chemistry, Federal University of Bahia (UFBA), Salvador, BA 40170-280, Brazil
³ São Carlos Institute of Physics (IFSC), University of São Paulo (USP), P.O. Box 369, São Carlos, SP 13566-590, Brazil; leoiwaki@yahoo.com.br (L.E.O.I.); chu@ifsc.usp.br (O.N.O.J.)
⁴ PPGQ, Center for Exact Sciences and Technology, Department of Chemistry, Federal University of São Carlos (UFSCar), São Carlos, SP 13565-905, Brazil
* Correspondence: lmercante@ufba.br (L.A.M.); daniel.correa@embrapa.br (D.S.C.)

Abstract: Bisphenol A (BPA) is an endocrine-disrupting chemical (EDC) employed in industrial processes that causes adverse effects on the environment and human health. Sensitive and inexpensive methods to detect BPA are therefore needed. In this paper, we describe an electrochemical biosensor for detecting low levels of BPA using polymeric electrospun nanofibers of polyamide 6 (PA6) and poly(allylamine hydrochloride) (PAH) decorated with gold nanoparticles (AuNPs), namely, PA6/PAH@AuNPs, which were deposited onto a fluorine-doped tin oxide (FTO) substrate. The hybrid layer was excellent for the immobilization of tyrosinase (Tyr), which allowed an amperometric detection of BPA with a limit of detection of 0.011 μM in the concentration range from 0.05 to 20 μM . Detection was also possible in real water samples with recoveries in the range of 92–105%. The improved sensing performance is attributed to the combined effect of the large surface area and porosity of PA6/PAH nanofibers, the catalytic activity of AuNPs, and oxidoreductase ability of Tyr. These results provide a route for novel biosensing architectures to monitor BPA and other EDCs in water resources.

Keywords: electrospinning; nanofibers; gold nanoparticles; tyrosinase; biosensor; endocrine disrupting compounds; bisphenol A



Citation: Mercante, L.A.; Iwaki, L.E.O.; Scagion, V.P.; Oliveira, O.N., Jr.; Mattoso, L.H.C.; Correa, D.S. Electrochemical Detection of Bisphenol A by Tyrosinase Immobilized on Electrospun Nanofibers Decorated with Gold Nanoparticles. *Electrochem* **2021**, *2*, 41–49. <https://doi.org/10.3390/electrochem2010004>

Academic Editor: Masato Sone

Received: 1 December 2020

Accepted: 19 January 2021

Published: 22 January 2021

Publisher's Note: MDPI stays neutral with regard to jurisdictional claims in published maps and institutional affiliations.



Copyright: © 2021 by the authors. Licensee MDPI, Basel, Switzerland. This article is an open access article distributed under the terms and conditions of the Creative Commons Attribution (CC BY) license (<https://creativecommons.org/licenses/by/4.0/>).

1. Introduction

The continuous discharge of highly toxic chemicals in the aquatic environment is a global concern due to their adverse effects on human health and the environment [1,2]. Pollutants with endocrine-disrupting activity, in particular, may damage the endocrine system of animals (including humans), even at such low concentrations as ng L^{-1} [3–5]. Regulatory agencies have established safe exposure limits, which are often low because the hormone systems are sensitive to these compounds [6–8]. Therefore, the demand for accurate, rapid and sensitive detection methods has been increasing with varied approaches to analyze endocrine-disrupting chemicals (EDCs) in various matrices [8–11]. Chemical (bio)sensors are advantageous over traditional analytical methods for this application owing to their high selectivity and sensitivity, fast analytical response, and possibility of automation, miniaturization, and integration [6,10]. One of the main features of these biosensors is that their architecture may be controlled with high precision upon combining nanomaterials and biomolecules.

Nanofibers have been demonstrated to work efficiently as platforms to immobilize biomolecules for further application in biosensing [12,13]. Among the various techniques

available for producing such nanofibers, electrospinning represents a unique technology that combines low cost, ease of production, and applicability for varied materials [12,14]. Electrospinning is based on an electrohydrodynamic process in which fibers ranging from nm to μm are produced by uniaxial electric stretching and elongation of a viscoelastic solution [12–14]. The nanofibrous membranes are featured with a high surface-to-volume ratio, interconnected porous structure, low barrier to diffusion, and adjustable functionality [12–15]. These properties enable the design of hybrid and composite nanofibrous-sensing films with remarkable sensitivity and selectivity for several analytes [16]. Furthermore, the nanofibrous structure is suitable to incorporate high loadings of enzymes, which is beneficial for biosensing performance [17–19]. Despite the suitability of electrospun nanofibers, considerable efforts are required to adjust the composition of the nanofibrous film to achieve a high performance for a given analyte.

Herein, we exploit a facile approach to fabricate enzyme-functionalized nanofibers to detect bisphenol A (2,2-bis(4-hydroxyphenyl) propane (BPA), one of the most important EDCs. Electrospun nanofibers of polyamide 6/poly(allylamine hydrochloride) (PA6/PAH) are decorated with gold nanoparticles (AuNPs), which then serve as a matrix for the immobilization of tyrosinase (Tyr). BPA detection is performed with an amperometric technique, including in real samples of water from different sources.

2. Materials and Methods

2.1. Materials

Polyamide 6 (PA6, $M_w = 20,000 \text{ g mol}^{-1}$), poly(allylamine hydrochloride) (PAH, $M_w = 15,000 \text{ g mol}^{-1}$), tyrosinase from mushroom (Tyr), hydrogen tetrachloroaurate (III) trihydrate ($\text{HAuCl}_4 \cdot 3\text{H}_2\text{O}$, $\geq 99.9\%$), sodium citrate, bovine serum albumin (BSA), N-hydroxysuccinimide (NHS), 1-ethyl-3-(3-dimethylaminopropyl)-carbodiimide (EDC), and bisphenol A were purchased from Sigma–Aldrich. Formic acid was purchased from Synth Chemical (São Paulo, Brazil). All aqueous solutions were prepared with double-distilled water, and the chemicals were used without further purification.

2.2. Fabrication of the Biosensing Platform

The sensing platform was prepared following a three-step process: (i) electrospinning of PA6/PAH, (ii) AuNP adsorption, and (iii) Tyr immobilization. The PA6/PAH solution was prepared by dissolving 20% (*w/v* with respect to the solvent) PA6 and 30% (*w/w* with respect to PA6) PAH in formic acid, with the resulting solution being stirred for 5 h at room temperature. The electrospun nanofibers were obtained by using an electrospinning apparatus at a feed rate of 0.01 mL h^{-1} and an electric voltage of 25 kV. A working distance of 10 cm was kept between the syringe and the metallic collector. The inner diameter of the steel needle was 0.7 mm. In order to ensure reproducibility in terms of electrochemical response, the nanofibers were collected with an optimized time of 10 min onto fluorine-doped tin oxide (FTO) glass substrates attached at the same position on the fiber collector system.

Citrate-stabilized AuNPs were synthesized with the Turkevich method [20], in which 20 mL of 1 mM HAuCl_4 was heated at 90°C and 2 mL of 1% sodium citrate solution was added under vigorous stirring and constant heating. During the addition, the yellow gold chloride solution turned to a red wine color, indicating the formation of the nanoparticles. The reaction was maintained for 30 min under gentle stirring and then cooled to room temperature. The formation of AuNPs, with an average size of $18 \pm 3 \text{ nm}$, was confirmed by ultraviolet-visible (UV–Vis) spectroscopy through the monitoring of the surface plasmon resonance absorption band at 520 nm. The electrospun nanofibers deposited on FTO were immersed into the AuNP solution, rinsed with distilled water, and dried under ambient conditions. Various adsorption times for AuNPs were tested (1, 6, 12, and 24 h) to determine the best electrochemical response for BPA, and the time period of 12 h was chosen for subsequent studies. Tyr was immobilized onto the PA6/PAH@AuNPs modified electrode by adding 20 μL of a solution containing 5 mM EDC and 5 mM NHS, which

acted as a cross-linker between the enzyme and the hybrid nanofibrous membrane [21,22]. Then, 10 μL of Tyr solution (2 mg mL^{-1} in 0.1 M PBS pH 7.0) was uniformly spread onto the PA6/PAH@AuNPs/FTO electrode and kept in a humid chamber for 12 h at 4 $^{\circ}\text{C}$. The modified electrode (PA6/PAH@AuNPs/Tyr/FTO) was washed thoroughly with PBS (0.1 M PBS pH 7.0) to remove any unbound enzyme, and then stored at 4 $^{\circ}\text{C}$.

2.3. Characterization and Electrochemical Measurements

The morphology of the PA6/PAH nanofibers was evaluated using a scanning electron microscope (SEM, JEOL 6510) operating at 10 kV, with the fiber diameter being estimated with an image analysis software (Image J, National Institutes of Health, Bethesda, MD, USA). In each experiment, the average fiber diameter was determined by measuring 100 random fibers using representative micrographs. After the decoration with AuNPs, the morphology was investigated using a field-emission gun scanning electron microscope (FEG-SEM, JEOL-JSM 6701F). The electrochemical experiments were performed using a PGSTAT30 Autolab electrochemical system (Metrohm) controlled with GPES software. The PA6/PAH@AuNPs/Tyr/FTO platform was used as the working electrode. A Pt foil and Ag/AgCl (3 M KCl) served as the counter (CE) and reference (RE) electrodes, respectively. Electrochemical characterization of modified electrodes was performed by cyclic voltammetry (CV) in a 0.05 M $[\text{Fe}(\text{CN})_6]^{3-/4-}$ solution containing 0.1 M KCl over a potential range from 0.1 to 0.6 V at a scan rate of 0.05 V s^{-1} . The electrochemical essay for BPA detection was performed using 0.01 M phosphate buffer solution (pH 7.0) at room temperature. To evaluate the activity of PA6/PAH@AuNPs/Tyr/FTO, cyclic voltammograms were acquired in the presence of BPA at the potential range from -0.2 to 0.4 V at a scan rate of 0.05 V s^{-1} . Chronoamperometric measurements were carried out under an applied potential of -0.1 V with successive addition of the BPA solution.

3. Results and Discussion

3.1. Choice of Materials for the Biosensing Platform

The materials used in this work were judiciously selected to leverage the characteristics of nanofibers, AuNPs, and Tyr, with which we expected to obtain a hybrid nanomaterial with improved electrochemical performance in BPA detection. To the best of our knowledge, this is the first use of hybrid electrospun nanofibers to immobilize tyrosinase for BPA detection. PA6 was chosen due to its nanofiber-forming ability and stability [23], while PAH was selected to introduce functional groups and improve adsorption of AuNPs via H-bonding and/or electrostatic interactions [24]. Citrate-capped AuNPs modified the nanofibers to enhance electrochemical performance, since AuNPs are capable of transferring electrons between the enzyme metal centers and the electrode, even achieving direct electron transfer [25]. The final hybrid nanomaterial offers functional groups ($-\text{NH}_2$ and $-\text{COO}^-$) and appropriate surface for enzyme immobilization through chemical bonding [22]. The cuproprotein enzyme Tyr was chosen for its ability to catalyze the oxidation of phenolic compounds, such as BPA. Furthermore, Tyr has higher specificity toward BPA than other polyphenol oxidases [25–27].

3.2. Characterization of the Biosensing Platform

Figure 1a,b show the scanning electron microscopy images of PA6/PAH and PA6/PAH@AuNPs nanofibers, respectively. Prior to the functionalization step, the PA6/PAH nanofibers (Figure 1a) showed a smooth and bead-free surface and an average diameter of 88 ± 24 nm. The FEG-SEM image in Figure 1b confirms that AuNPs were attached homogeneously onto PA6/PAH nanofibers, which is beneficial for sensing performance [28]. The stability of the decorated nanofiber was evaluated by leaching tests in water, which revealed that the AuNPs were strongly attached to the nanofiber surface. Citrate-functionalized AuNPs may interact with PA6/PAH through H-bonding and/or electrostatic forces [22,24]. H-bonding should occur between amide groups from PA6, or

amine groups from PAH, and the carboxylic groups from the functionalized AuNPs, while the latter may interact electrostatically with PAH (pKa 8.7).

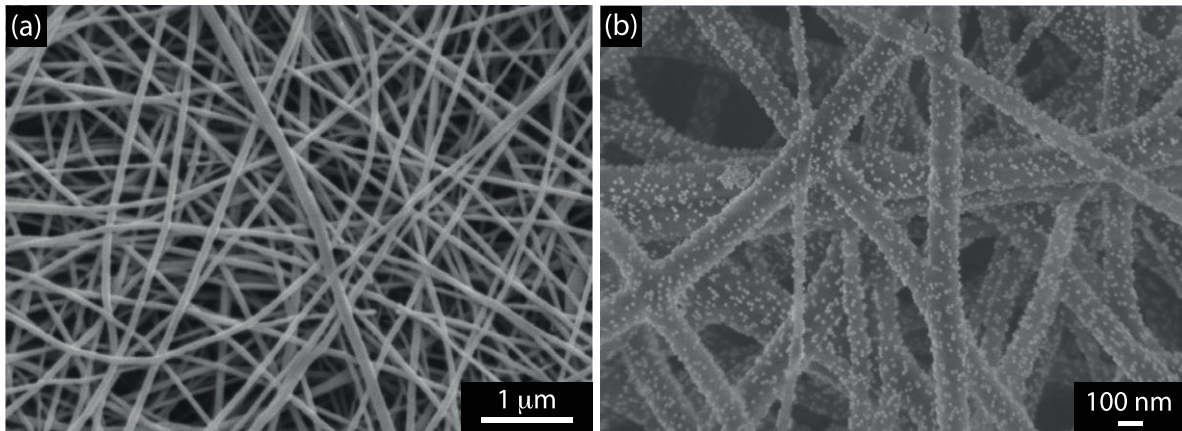


Figure 1. (a) SEM image of PA6/PAH and (b) FEG-SEM image of PA6/PAH@AuNPs nanofibers.

The electrochemical characterization of the electrodes was performed using cyclic voltammetry, which results are shown in Figure 2. A well-defined redox peak was observed for bare FTO with peak separation (ΔE_p) of 122 mV. Upon modifying the electrode with PA6/PAH@AuNPs, the redox current increased and ΔE_p decreased to 115 mV, implying an increase in the electroactive area of bare FTO. The chemical immobilization of Tyr was accompanied by a decrease in the peak current since the enzyme blocked electron transport with its insulating nature [27]. The voltammogram for the Tyr-modified electrode (blue curve in Figure 2) was used to calculate the average surface concentration of ionic species (Γ), following Equation (1) [21,29]:

$$\Gamma = (4RTI_p)/(n^2F^2A\nu) \quad (1)$$

where R is the universal gas constant, T is the temperature (K), I_p is the peak current, n is the number of electrons, F is the Faraday constant, A is the electrode surface area (cm^2), and ν is the scan rate (Vs^{-1}). The surface concentration of electrochemically active species adsorbed onto the electrode was estimated as $3.72 \times 10^{-9} \text{ mol cm}^{-2}$.

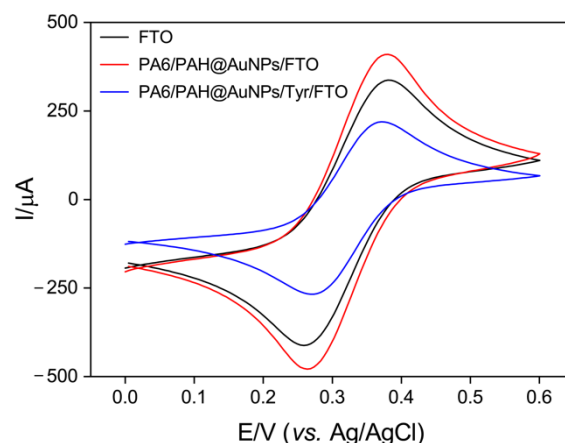


Figure 2. CV curves of FTO, PA6/PAH@AuNPs/FTO, and PA6/PAH@AuNPs/Tyr/FTO using a 0.05 M $[\text{Fe}(\text{CN})_6]^{3-/4-}$ solution containing 0.1 M KCl.

3.3. Electrochemical Detection of BPA

The electrochemical behavior of BPA at the interface of the PA6/PAH@AuNPs/Tyr-modified electrode was investigated using the CV technique. Figure 3 displays a large

irreversible peak upon adding BPA. The reduction reaction took place at the modified electrode interface at a low potential (0.1 V) and the peak current increased due to the increase in BPA concentration. In addition, a slight change in the oxidation region can be observed with the addition of BPA, which might be attributed to the BPA oxidation. Similar behavior was observed in previous studies [30,31]. Tyr is a binuclear copper-containing enzyme that catalyzes the hydroxylation and oxidation of phenolic compounds to *o*-quinones [25]. The most accepted mechanism for BPA electrooxidation consists of the transfer of two electrons and two protons [25,32] in the presence of dissolved oxygen, as indicated in Equation (2) through (4): tyrosinase catalyzes the oxidation of phenolic compounds to *o*-quinone derivatives via catechol derivatives. The generated *o*-quinone can be electrochemically reduced at a low potential [33]. The reduction signal of *o*-quinone is normally used to determine the phenolic compound with the purpose of preventing interference [31,33].

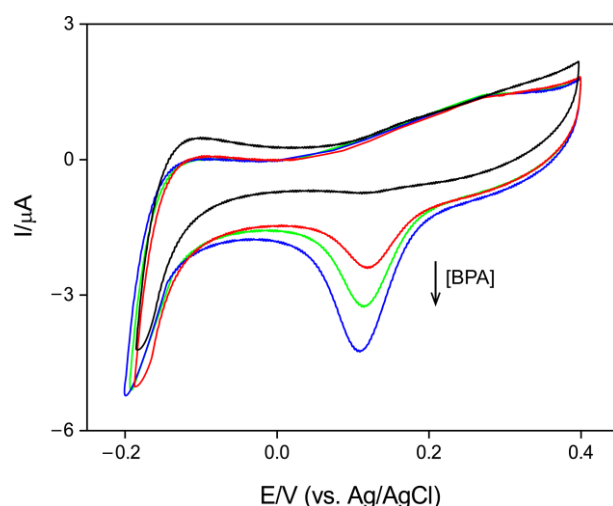
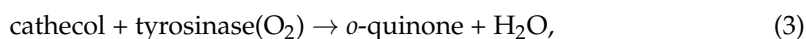
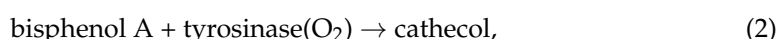


Figure 3. CV curves of PA6/PAH@AuNPs/Tyr/FTO in 0.01 M PBS (pH 7.0) with successive addition of BPA. Scan rate: 0.05 V s^{-1} .

Chronoamperometry was used to investigate the performance of the biosensor in determining BPA. Figure 4 shows a linear relationship between the peak current and the log of BPA concentrations, with the regression equation $\Delta I (\mu\text{A}) = 1.79 \log [\text{BPA}] + 3.98$ ($R^2 = 0.997$). The limit of detection (LOD), calculated according to $S/N = 3$ criterion, was $0.011 \mu\text{M}$. The reproducibility and repeatability of the PA6/PAH@AuNPs/Tyr electrode were evaluated by performing repeated experiments with solutions containing $5 \mu\text{M}$ BPA. For ten successive measurements, the relative standard deviation (RSD) was 2.9% for a given electrode, while it increased to 7.6% when three nominally identical electrodes were used. Note in Figure 4 that the response curve tended to reach a plateau for concentrations above $20 \mu\text{M}$, indicating typical Michaelis–Menten enzyme kinetics. The apparent Michaelis–Menten constant (K_m) was 0.34 mM , lower than the K_m of the free enzyme (1.46 mM) reported for the BPA substrate [34]. This low K_m indicates that Tyr retains its bioactivity after chemical immobilization on the hybrid nanofiber and has a high affinity for BPA [18,35].

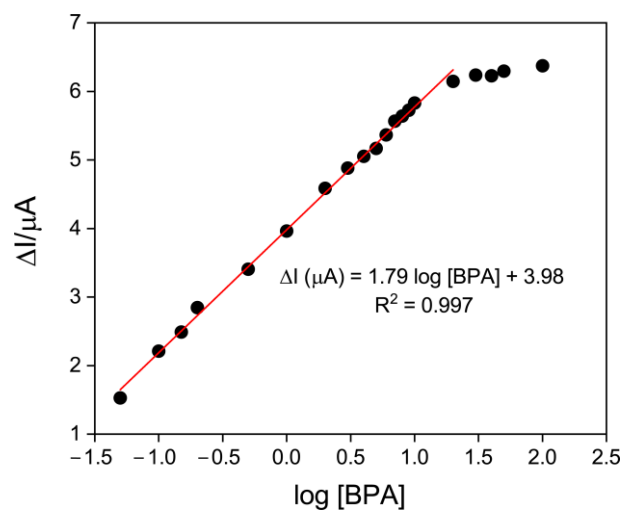


Figure 4. Calibration curve for BPA detection for the PA6/PAH@AuNPs/Tyr/FTO electrode, with the corresponding linear fitting.

The performance of the PA6/PAH@AuNPs/Tyr/FTO biosensor is compared with other BPA sensors in Table 1. Its competitive limit of detection (LOD) and wider linear range compared to other sensing platforms are ascribed to the synergy between the nanofibrous structure and AuNPs and inherent compatibility of the components. Furthermore, the immobilization of the Tyr enzyme proved effective for sensitive detection of BPA, as demonstrated with the lower LOD of PA6/PAH@AuNPs/Tyr than with other enzyme-free nanofiber-based electrochemical sensors [36,37]. In addition, our work opens the possibility for developing multifunctional nanofibers as tyrosinase-based nanofibrous membranes have been applied for BPA removal [34].

Table 1. Comparison of nanomaterial-based tyrosinase electrochemical biosensors for BPA detection.

Electrode	Nanomaterial Type	Linear Range (μM)	LOD (μM)	Reference
Tyr-NGP-Chi/GCE	Carbon-based	0.1–2	0.033	[38]
Tyr-GDY-Chi/GCE	Carbon-based	0.1–3.5	0.024	[27]
Tyr/Mag-BCNPs-COOH/MGCE	Nanocomposite	0.01–1.01	0.003	[26]
Tyr-SF-MWNTs-CoPc/GCE	Nanocomposite	0.05–3	0.03	[35]
CuMOF-Tyr-Chi/GCE	Nanocomposite	0.05–3	0.013	[39,40]
Tyr@PANI-Mn ₃ O ₄ /ITO	Nanocomposite	0.004–0.8	0.004	[41]
Tyr-NiNPs/SPCE	Metallic Nanoparticle	0.9–48	0.007	[30]
Tyr/SnNP/GCE	Metallic Nanoparticle	0.01–0.1	0.002	[42]
Nafion/Tyr/Au/SPCE	Metallic Nanoparticle	0.5–50	0.077	[32]
nTyr-Chi/GCE	Nanocapsule	0.05–2	0.012	[43]
BCNPs/Tyr/Nafion/GCE	Polymeric Nanoparticle	0.02–10	0.003	[44]
PA6/PAH@AuNPs/Tyr/FTO	Electrospun Nanofiber	0.05–20	0.011	This work

Note: NGP–nanographene; Chi–chitosan; GCE–glassy carbon electrode; GDY–graphdiyne; Mag-BCNPs-COOH–magnetic biochar nanoparticles; MGCE–magnetic glassy carbon electrode; SF–silk fibroin; MWNTs–carbon nanotubes; CoPc–cobalt phthalocyanine; CuMOF–copper-centered metal-organic framework; PANI–polyaniline; ITO–indium tin oxide; SPCE–screen-printed carbon electrode; nTyr–tyrosinase nanocapsules; BCNPs–sugarcane-derived biochar nanoparticle.

The possible interference from potential interferents in the detection of BPA was investigated, and the results are present in Table 2. One notices that the co-presence of 100-fold concentrations of ascorbic acid, uric acid, urea, glucose, KCl, and NaCl did not interfere in the detection. Also evaluated was BPA detection in the presence of other phenolic compounds, since Tyr is known to possess activity in these compounds [45]. As indicated in Table 2, the maximum interference was around 20% for phenol, and therefore the ability to detect BPA specifically was preserved.

Table 2. Selectivity of the amperometric PA6/PAH@AuNPs/Tyr biosensor for BPA.

Compound	Concentration (μM)	% of Signal
BPA	5	100
phenol	20	20.5
4-nitrophenol	20	7.6
4-methoxyphenol	20	4.7
4-aminophenol	20	1.5
ascorbic acid, uric acid, urea, glucose, KCl, NaCl	500	-

The feasibility and reliability of the biosensor were estimated by evaluating the recovery of BPA in real samples. Water samples of different origins (bottled water, tap water, and river water), without pretreatment, were spiked with 5 μM BPA and the percentage recoveries were calculated. Table 3 displays recoveries ranging from 92 to 105% with an RSD of 1.3–4.1%, indicating that the PA6/PAH@AuNPs/Tyr platform may be applied to determine BPA in real samples.

Table 3. Determination of BPA in real water samples ($n = 3$).

Real Sample	Recovery (%)	RSD (%)
Tap Water	95	1.3
Bottled Water	105	2.7
River Water	92	4.1

4. Conclusions

A novel approach using Tyr-immobilized hybrid nanofibrous mats in electrochemical biosensors to detect BPA is reported here for the first time. Owing to the synergy of the materials employed, namely, nanofibers decorated with AuNPs for the immobilization of Tyr, the sensing performance was superior to similar biosensors reported in the literature. The limit of detection was 0.011 μM , with a wide linear range from 0.05 to 20 μM . The biosensors were reproducible and robust and could detect BPA in water samples from different sources, including tap and river water. It is significant that the chemical immobilization of Tyr onto a hybrid PA6/PAH@Au nanofibrous sensing layer provides an alternative and simple strategy to detect BPA with high sensitivity, which can also be explored for other endocrine disruptors. Furthermore, the concepts behind the novel architecture may be exploited in the design of multifunctional materials that combine both removal and detection functions.

Author Contributions: Conceptualization, L.A.M., L.E.O.I. and D.S.C.; investigation, L.A.M., L.E.O.I. and V.P.S.; writing-original draft preparation, L.A.M.; writing-review and editing, L.A.M., L.E.O.I., O.N.O.J., V.P.S., L.H.C.M. and D.S.C.; funding acquisition, O.N.O.J., L.H.C.M. and D.S.C.; supervision, O.N.O.J., L.H.C.M. and D.S.C. All authors have read and agreed to the published version of the manuscript.

Funding: This research was funded by FAPESP (2017/12174-4, 2018/22214-6), CNPq, CAPES, MCTI-SisNano (CNPq/402.287/2013-4), and Rede Agronano-EMBRAPA from Brazil.

Institutional Review Board Statement: Not applicable.

Informed Consent Statement: Not applicable.

Data Availability Statement: The data presented in this study are available from the corresponding author upon request.

Conflicts of Interest: The authors declare no conflict of interest.

References

1. Simón-Herrero, C.; Naghdi, M.; Taheran, M.; Kaur Brar, S.; Romero, A.; Valverde, J.L.; Avalos Ramirez, A.; Sánchez-Silva, L. Immobilized laccase on polyimide aerogels for removal of carbamazepine. *J. Hazard. Mater.* **2019**, *376*, 83–90. [[CrossRef](#)]
2. Koloti, L.E.; Gule, N.P.; Arotiba, O.A.; Malinga, S.P. Laccase-immobilized dendritic nanofibrous membranes as a novel approach towards the removal of bisphenol A. *Environ. Technol.* **2018**, *39*, 392–404. [[CrossRef](#)] [[PubMed](#)]
3. Maynard, I.F.N.; Cavalcanti, E.B.; da Silva, L.L.; Martins, E.A.J.; Pires, M.A.F.; de Barros, M.L.; Cardoso, E.; Marques, M.N. Assessing the presence of endocrine disruptors and markers of anthropogenic activity in a water supply system in northeastern Brazil. *J. Environ. Sci. Heal. Part A Toxic Hazard. Subst. Environ. Eng.* **2019**, *54*, 891–898. [[CrossRef](#)]
4. Maryšková, M.; Schaabová, M.; Tománková, H.; Novotný, V.; Rysová, M. Wastewater Treatment by Novel Polyamide/Polyethylenimine Nanofibers with Immobilized Laccase. *Water* **2020**, *12*, 588. [[CrossRef](#)]
5. Starling, M.C.V.M.; Amorim, C.C.; Leão, M.M.D. Occurrence, control and fate of contaminants of emerging concern in environmental compartments in Brazil. *J. Hazard. Mater.* **2019**, *372*, 17–36. [[CrossRef](#)] [[PubMed](#)]
6. Ali, M.Y.; Alam, A.U.; Howlader, M.M.R. Fabrication of highly sensitive Bisphenol A electrochemical sensor amplified with chemically modified multiwall carbon nanotubes and β -cyclodextrin. *Sens. Actuators B Chem.* **2020**, *320*, 128319. [[CrossRef](#)]
7. Sinha, A.; Wu, L.; Lu, X.; Chen, J.; Jain, R. Advances in sensing and biosensing of bisphenols: A review. *Anal. Chim. Acta* **2018**, *998*, 1–27. [[CrossRef](#)]
8. Kaya, S.I.; Cetinkaya, A.; Bakirhan, N.K.; Ozkan, S.A. Trends in sensitive electrochemical sensors for endocrine disruptive compounds. *Trends Environ. Anal. Chem.* **2020**, *28*, e00106. [[CrossRef](#)]
9. Ragavan, K.V.; Rastogi, N.K.; Thakur, M.S. Sensors and biosensors for analysis of bisphenol-A. *TrAC Trends Anal. Chem.* **2013**, *52*, 248–260. [[CrossRef](#)]
10. Tajik, S.; Beitollahi, H.; Nejad, F.G.; Zhang, K.; Van Le, Q.; Jang, H.W.; Kim, S.Y.; Shokouhimehr, M. Recent Advances in Electrochemical Sensors and Biosensors for Detecting Bisphenol A. *Sensors* **2020**, *20*, 3364. [[CrossRef](#)]
11. Lu, X.; Sun, J.; Sun, X. Recent advances in biosensors for the detection of estrogens in the environment and food. *TrAC Trends Anal. Chem.* **2020**, *127*, 115882. [[CrossRef](#)]
12. Andre, R.S.; Mercante, L.A.; Facure, M.H.M.; Pavinatto, A.; Correa, D.S. Electrospun composite nanofibers as sensors for food analysis. In *Electrospun Polymers and Composites*; Elsevier: Amsterdam, The Netherlands, 2021; pp. 261–286. ISBN 9780128196113.
13. Sapountzi, E.; Braiek, M.; Chateaux, J.-F.; Jaffrezic-Renault, N.; Lagarde, F. Recent Advances in Electrospun Nanofiber Interfaces for Biosensing Devices. *Sensors* **2017**, *17*, 1887. [[CrossRef](#)] [[PubMed](#)]
14. Mercante, L.A.; Scagion, V.P.; Migliorini, F.L.; Mattoso, L.H.C.; Correa, D.S. Electrospinning-based (bio)sensors for food and agricultural applications: A review. *TrAC Trends Anal. Chem.* **2017**, *91*, 91–103. [[CrossRef](#)]
15. Li, Y.; Abedalwafa, M.A.; Tang, L.; Li, D.; Wang, L. Electrospun Nanofibers for Sensors. In *Electrospinning: Nanofabrication and Applications*; Elsevier: Amsterdam, The Netherlands, 2019; pp. 571–601. ISBN 9780323512701.
16. Yang, T.; Zhan, L.; Huang, C.Z. Recent insights into functionalized electrospun nanofibrous films for chemo-/bio-sensors. *TrAC Trends Anal. Chem.* **2020**, *124*, 115813. [[CrossRef](#)]
17. Jankowska, K.; Zdarta, J.; Grzywaczyk, A.; Kijeńska-Gawrońska, E.; Biadasz, A.; Jesionowski, T. Electrospun poly(methyl methacrylate)/polyaniline fibres as a support for laccase immobilisation and use in dye decolourisation. *Environ. Res.* **2020**, *184*, 109332. [[CrossRef](#)] [[PubMed](#)]
18. Smith, S.; Goodge, K.; Delaney, M.; Struzyk, A.; Tansey, N.; Frey, M. A Comprehensive Review of the Covalent Immobilization of Biomolecules onto Electrospun Nanofibers. *Nanomaterials* **2020**, *10*, 2142. [[CrossRef](#)]
19. Fatarella, E.; Spinelli, D.; Ruzzante, M.; Pogni, R. Nylon 6 film and nanofiber carriers: Preparation and laccase immobilization performance. *J. Mol. Catal. B Enzym.* **2014**, *102*, 41–47. [[CrossRef](#)]
20. Kimling, J.; Maier, M.; Okenve, B.; Kotaidis, V.; Ballot, H.; Plech, A. Turkevich method for gold nanoparticle synthesis revisited. *J. Phys. Chem. B* **2006**, *110*, 15700–15707. [[CrossRef](#)]
21. Mercante, L.A.; Facure, M.H.M.; Sanfelice, R.C.; Migliorini, F.L.; Mattoso, L.H.C.; Correa, D.S. One-pot preparation of PEDOT:PSS-reduced graphene decorated with Au nanoparticles for enzymatic electrochemical sensing of H₂O₂. *Appl. Surf. Sci.* **2017**, *407*, 162–170. [[CrossRef](#)]
22. Soares, J.C.; Iwaki, L.E.O.; Soares, A.C.; Rodrigues, V.C.; Melendez, M.E.; Fregnani, J.H.T.G.; Reis, R.M.; Carvalho, A.L.; Corrêa, D.S.; Oliveira, O.N. Immunosensor for Pancreatic Cancer Based on Electrospun Nanofibers Coated with Carbon Nanotubes or Gold Nanoparticles. *ACS Omega* **2017**, *2*, 6975–6983. [[CrossRef](#)]
23. Migliorini, F.L.; Sanfelice, R.C.; Pavinatto, A.; Steffens, J.; Steffens, C.; Correa, D.S. Voltammetric cadmium(II) sensor based on a fluorine doped tin oxide electrode modified with polyamide 6/chitosan electrospun nanofibers and gold nanoparticles. *Microchim. Acta* **2017**, *184*, 1077–1084. [[CrossRef](#)]
24. Mercante, L.A.; Pavinatto, A.; Iwaki, L.E.O.; Scagion, V.P.; Zucolotto, V.; Oliveira, O.N.; Mattoso, L.H.C.; Correa, D.S. Electrospun polyamide 6/poly(allylamine hydrochloride) nanofibers functionalized with carbon nanotubes for electrochemical detection of dopamine. *ACS Appl. Mater. Interfaces* **2015**, *7*, 4784–4790. [[CrossRef](#)] [[PubMed](#)]
25. Raymundo-Pereira, P.A.; Silva, T.A.; Caetano, F.R.; Ribovski, L.; Zapp, E.; Brondani, D.; Bergamini, M.F.; Marcolino, L.H.; Banks, C.E.; Oliveira, O.N.; et al. Polyphenol oxidase-based electrochemical biosensors: A review. *Anal. Chim. Acta* **2020**, *1139*, 198–221. [[CrossRef](#)] [[PubMed](#)]

26. He, L.; Yang, Y.; Kim, J.; Yao, L.; Dong, X.; Li, T.; Piao, Y. Multi-layered enzyme coating on highly conductive magnetic biochar nanoparticles for bisphenol A sensing in water. *Chem. Eng. J.* **2020**, *384*, 123276. [[CrossRef](#)]
27. Wu, L.; Gao, J.; Lu, X.; Huang, C.; Chen, J. Graphdiyne: A new promising member of 2D all-carbon nanomaterial as robust electrochemical enzyme biosensor platform. *Carbon N. Y.* **2020**, *156*, 568–575. [[CrossRef](#)]
28. Wang, H.; Wang, D.; Peng, Z.; Tang, W.; Li, N.; Liu, F. Assembly of DNA-functionalized gold nanoparticles on electrospun nanofibers as a fluorescent sensor for nucleic acids. *Chem. Commun.* **2013**, *49*, 5568–5570. [[CrossRef](#)]
29. Pavinatto, A.; Mercante, L.A.; Facure, M.H.M.; Pena, R.B.; Sanfelice, R.C.; Mattoso, L.H.C.; Correa, D.S. Ultrasensitive biosensor based on polyvinylpyrrolidone/chitosan/reduced graphene oxide electrospun nanofibers for 17 α -ethinylestradiol electrochemical detection. *Appl. Surf. Sci.* **2018**, *458*, 431–437. [[CrossRef](#)]
30. Alkadir, R.S.J.; Ganesana, M.; Won, Y.-H.; Stanciu, L.; Andreescu, S. Enzyme functionalized nanoparticles for electrochemical biosensors: A comparative study with applications for the detection of bisphenol A. *Biosens. Bioelectron.* **2010**, *26*, 43–49. [[CrossRef](#)]
31. Oriero, D.A.; Gyan, I.O.; Bolshaw, B.W.; Cheng, I.F.; Aston, D.E. Electrospun biocatalytic hybrid silica-PVA-tyrosinase fiber mats for electrochemical detection of phenols. *Microchem. J.* **2015**, *118*, 166–175. [[CrossRef](#)]
32. Inroga, F.A.D.; Rocha, M.O.; Lavayen, V.; Arguello, J. Development of a tyrosinase-based biosensor for bisphenol A detection using gold leaf-like microstructures. *J. Solid State Electrochem.* **2019**, *23*, 1659–1666. [[CrossRef](#)]
33. Zehani, N.; Fortgang, P.; Saddek Lachgar, M.; Baraket, A.; Arab, M.; Dzyadevych, S.V.; Kherrat, R.; Jaffrezic-Renault, N. Highly sensitive electrochemical biosensor for bisphenol A detection based on a diazonium-functionalized boron-doped diamond electrode modified with a multi-walled carbon nanotube-tyrosinase hybrid film. *Biosens. Bioelectron.* **2015**, *74*, 830–835. [[CrossRef](#)] [[PubMed](#)]
34. Zdarta, J.; Staszak, M.; Jankowska, K.; Kaźmierczak, K.; Degórska, O.; Nguyen, L.N.; Kijeńska-Gawrońska, E.; Pinelo, M.; Jesionowski, T. The response surface methodology for optimization of tyrosinase immobilization onto electrospun polycaprolactone-chitosan fibers for use in bisphenol A removal. *Int. J. Biol. Macromol.* **2020**, *165*, 2049–2059. [[CrossRef](#)] [[PubMed](#)]
35. Yin, H.; Zhou, Y.; Xu, J.; Ai, S.; Cui, L.; Zhu, L. Amperometric biosensor based on tyrosinase immobilized onto multiwalled carbon nanotubes-cobalt phthalocyanine-silk fibroin film and its application to determine bisphenol A. *Anal. Chim. Acta* **2010**, *659*, 144–150. [[CrossRef](#)] [[PubMed](#)]
36. Furquim, F.C.; Santos, E.N.; Mercante, L.A.; Amaral, M.M.; Pavinatto, A.; Rodrigues, B.V.M. Green and low-cost electrospun membranes from polycaprolactone/graphene oxide for Bisphenol A sensing. *Mater. Lett.* **2020**, *274*, 128014. [[CrossRef](#)]
37. Sun, J.; Liu, Y.; Lv, S.; Huang, Z.; Cui, L.; Wu, T. An Electrochemical Sensor Based on Nitrogen-doped Carbon Nanofiber for Bisphenol A Determination. *Electroanalysis* **2016**, *28*, 439–444. [[CrossRef](#)]
38. Wu, L.; Deng, D.; Jin, J.; Lu, X.; Chen, J. Nanographene-based tyrosinase biosensor for rapid detection of bisphenol A. *Biosens. Bioelectron.* **2012**, *35*, 193–199. [[CrossRef](#)]
39. Wang, X.; Lu, X.; Wu, L.; Chen, J. 3D metal-organic framework as highly efficient biosensing platform for ultrasensitive and rapid detection of bisphenol A. *Biosens. Bioelectron.* **2015**, *65*, 295–301. [[CrossRef](#)]
40. Lu, X.; Wang, X.; Wu, L.; Wu, L.; Fu, L.; Gao, Y.; Chen, J. Response Characteristics of Bisphenols on a Metal-Organic Framework-Based Tyrosinase Nanosensor. *ACS Appl. Mater. Interfaces* **2016**, *8*, 16533–16539. [[CrossRef](#)]
41. Singh, N.; Ali, M.A.; Suresh, K.; Agrawal, V.V.; Rai, P.; Sharma, A.; Malhotra, B.D.; John, R. In-situ electrosynthesized nanostructured Mn₃O₄-polyaniline nanofibers- biointerface for endocrine disrupting chemical detection. *Sens. Actuators B Chem.* **2016**, *236*, 781–793. [[CrossRef](#)]
42. Mayedwa, N.; Ajayi, R.F.; Mongwaketsi, N.; Matinise, N.; Mulaudzi-Masuku, T.; Hendricks, K.; Maaza, M. Development of a Novel Tyrosinase Amperometric Biosensor Based on Tin Nanoparticles for the Detection of Bisphenol A (4,4-Isopropylidenediphenol) in Water. *J. Phys. Conf. Ser.* **2019**, *1310*, 012005. [[CrossRef](#)]
43. Wu, L.; Lu, X.; Niu, K.; Chen, J. Tyrosinase nanocapsule based nano-biosensor for ultrasensitive and rapid detection of bisphenol A with excellent stability in different application scenarios. *Biosens. Bioelectron.* **2020**, *165*, 112407. [[CrossRef](#)] [[PubMed](#)]
44. Liu, Y.; Yao, L.; He, L.; Liu, N.; Piao, Y. Electrochemical Enzyme Biosensor Bearing Biochar Nanoparticle as Signal Enhancer for Bisphenol A Detection in Water. *Sensors* **2019**, *19*, 1619. [[CrossRef](#)] [[PubMed](#)]
45. Min, K.; Park, G.W.; Yoo, Y.J.; Lee, J.S. A perspective on the biotechnological applications of the versatile tyrosinase. *Bioresour. Technol.* **2019**, *289*, 121730. [[CrossRef](#)] [[PubMed](#)]